National Conference with International Participation
ENGINEERING MECHANICS 2006
Svratka, Czech Republic, May 15 – 18, 2006
paper no. 291

EVALUATION OF GEOMETRICAL PROPERTIES OF AGGREGATE PARTICLES

D. Rypl [1]

Summary: *The present paper deals with the evaluation of geometrical properties of aggregate particles. Initially, a smooth representation of the aggregate particle shape is recovered from its digital voxel based representation using the expansion into spherical harmonic functions. The resolution of the smooth representation can be flexibly controlled by the number of terms in the expansion. Then the geometrical properties, including volume, surface area, moments of inertia, and curvature, are evaluated using numerical integration of appropriate analytical terms. The advantage of this approach consists in the fact that it unifies the approach for the evaluation of geometrical properties and that it allows to evaluate important properties such as the curvature or surface area, which cannot be reliably assessed from the digital representation. The evaluated geometrical properties may be used to classify aggregate from different sources, according to their shape and size.*

1. Introduction

The design of concrete with specified properties became of increasing importance with the wide use of high-performance concretes (HPCs), such as pumpable concrete or self compacting concrete (SCC). Many concrete properties, starting from the mechanical properties as the compressive strength and modulus of elasticity, over the rheological properties influencing the workability of fresh concrete, up to physical properties as diffusivity and thermal and electric conductivity, for example, are dependent on the shape and consequently also on the geometrical properties of aggregate particles. However, accurate evaluation of these geometrical properties is not straightforward due to rather difficult mathematical characterization of aggregate particles of random shape. The realistic description of random particles is therefore a necessary prerequisite for proper evaluation of geometrical properties of aggregate particles and for their incorporation into computational models representing concrete as a multiscale random composite material with realistically described aggregates.

Modern tomographic scanning devices offer a powerful nondestructive technique for the digital description of opaque solid objects. However, the resulting voxel based representation of the object is not always appropriate for further processing. Huge amount of data related to digital images of high resolution makes dealing with this representation quite cumbersome and

[1] Doc. Dr. Ing. Daniel Rypl, Department of Mechanics, Faculty of Civil Engineering, Czech Technical University in Prague, Thákurova 7, 166 29, Prague 6, Czech Republic, tel. +420 224 354 369, e-mail drypl@fsv.cvut.cz

its step-wise character complicates its integration into computational models. In the present work, the digital representation is first used to derive a smooth representation of the aggregate particle using the expansion into spherical harmonic functions [Garboczi 2002]. Although this representation is not universal (it implies that the aggregate particle is of star-like shape with no internal voids) it is suitable for almost all aggregates used in structural concrete. The significant advantage of this approach is that the resolution of the smooth representation can be flexibly controlled (within the resolution of the original digital representation) by the number of terms in the expansion and that it allows to describe aggregate particles by relatively low number of parameters. This makes this technique attractive for computational models handling large number of aggregate particles. Moreover, the smooth representation enables also a simple evaluation of many geometrical properties of aggregate particles which can be used to build aggregate databases.

The paper is organized as follows. Initially, a simple digital representation of the aggregate particle is outlined in Section 2. Its mathematical description based on the spherical harmonic analysis is then recalled in Section 3. In Section 4, the evaluation of individual geometrical properties based on the spherical harmonic expansion is outlined. The technique is then verified on a few examples in Section 5. The paper ends with concluding remarks in Section 6.

2. Digital Representation of Aggregate Particle

The three-dimensional digital representation that comes out from tomographic scanning can be interpreted as the sequence of two-dimensional gray scale digital images corresponding to (but not necessarily physically taken at) parallel cuts through a three-dimensional object. Each digital image consists of the grid of pixels of gray scale value related to a specific property.

In the case of the description of the shape of aggregate particles, the gray scale images can be thresholded to black and white images, in which (let's say) the black pixels correspond to the aggregate itself and the white pixels represent its surroundings. Assuming that the pixel in each image is of the shape of a square and that the individual cuts are at the distance corresponding to the edge length of that square, then each aggregate particle is described by a set of black cubes (voxels). Depending on the resolution (the physical size of the pixel), such a voxel based representation is either too coarse (of low resolution), probably inappropriate for further processing or sufficiently fine (of adequate or high resolution) which is appropriate for further processing but at the cost of handling huge amount of data. An example of digital representation of a particular aggregate particle for two different resolutions is depicted in Figure 1.

The digital representation suffers, besides the resolution demands and consequently also the memory demands, from other drawbacks. It is well known that quantities corresponding to the spatial dimension of the digital representation (dimension 3 in the case of voxel based representation) can be assessed with the accuracy depending on the resolution. However, this is not true for quantities of lower dimension, for example the surface area. Moreover, due to the step-wise character, the digital representation does not allow to evaluate some quantities at all, for example the curvature. This is considered as significant bottleneck especially with respect to the integration of aggregate particles into computational models which require appropriate spatial discretization of particles, because the curvature based control, serving as an efficient tool decreasing the discretization error and ensuring maintaining the volume fraction of particles, is simply not available.

It is therefore apparent, that an alternative description handling geometrical shapes with much smaller amount of data and allowing precise evaluation of various quantities is desirable.

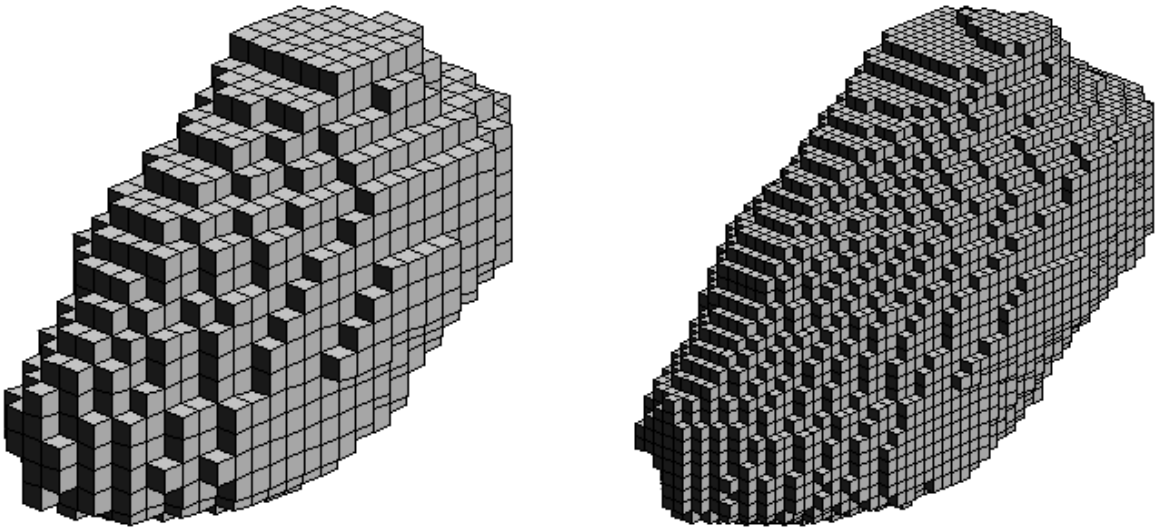

Figure 1: Digital representation of the aggregate particle for a lower (left) and higher (right) resolution (only the voxels corresponding to the aggregate are shown).

The mathematical description based on the spherical harmonic analysis [Garboczi 2002] seems to be a good choice.

3. Mathematical Representation of Aggregate Particle

In the mathematical representation, the individual particles are described by a scalar function $r(\eta,\varphi)$, defined as the distance of the particle surface point from the particle center of mass measured in the direction of spherical coordinates η and φ with the origin located in the particle center of mass (see Figure 2). The Cartesian coordinates of the surface point (components of its position vector $\boldsymbol{r}$) are then given by

$$x(\eta,\varphi) = r(\eta,\varphi)\sin(\eta)\cos(\varphi)\ , \tag{1}$$

$$y(\eta,\varphi) = r(\eta,\varphi)\sin(\eta)\sin(\varphi)\ , \tag{2}$$

$$z(\eta,\varphi) = r(\eta,\varphi)\cos(\eta)\ . \tag{3}$$

If the function $r(\eta,\varphi)$ is smooth on unit sphere ($0\leq\eta\leq\pi, 0\leq\varphi\leq 2\pi$) and periodic in φ, it can be expressed in the form of the expansion into spherical harmonic functions as

$$r(\eta,\varphi) = \sum_{n=0}^{\infty}\sum_{m=-n}^{n} a_{nm}Y_n^m(\eta,\varphi)\ , \tag{4}$$

where a_{nm} are yet unknown coefficients of the expansion and $Y_n^m(\eta,\varphi)$ are the spherical harmonic functions defined by

$$Y_n^m(\eta,\varphi) = f_{nm}P_n^m(\cos(\eta))(\cos(m\varphi) + i\sin(m\varphi))\ , \tag{5}$$

where

$$f_{nm} = \sqrt{\frac{2n+1}{4\pi}\frac{(n-m)!}{(n+m)!}}\ . \tag{6}$$

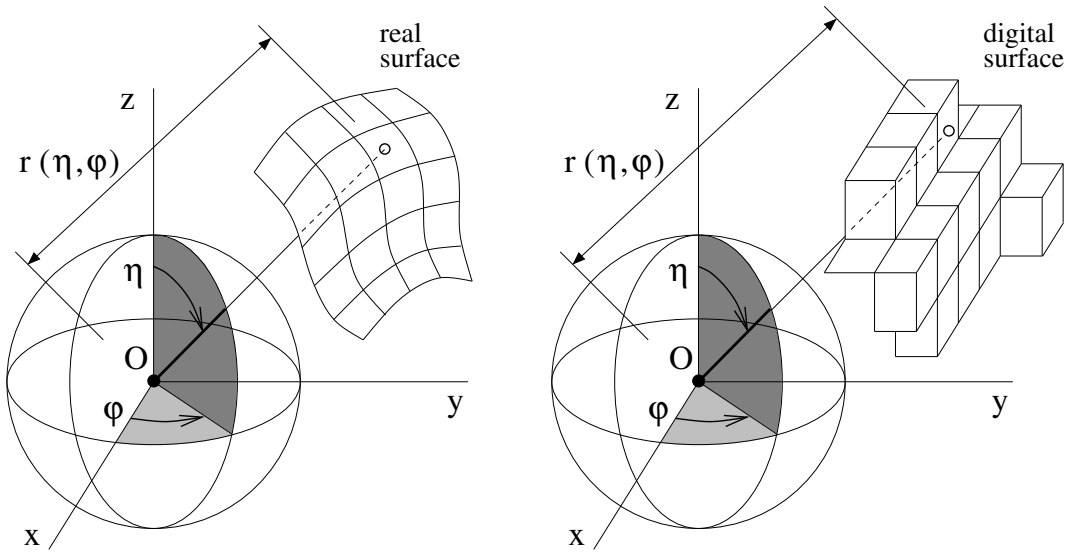

Figure 2: Description of the aggregate particle in the spherical coordinate system.

The associated Legendre polynomials $P_n^m(x)$ can be expressed via the ordinary Legendre polynomials $P_n(x)$ in the form

$$P_n^m(x) = \sqrt{(1-x^2)^m}\frac{d^m P_n(x)}{dx^m} \; . \tag{7}$$

It is however more convenient to evaluate $P_n^m(x)$ from recursive relations [Weisstein]

$$P_n^n(x) = (2n-1)!!\sqrt{(1-x^2)^n} \; , \tag{8}$$

$$P_{n+1}^n(x) = x(2n+1)P_n^n(x) \; , \tag{9}$$

$$(n-m)P_n^m(x) = x(2n-1)P_{n-1}^m(x) - (n+m-1)P_{n-2}^m(x) \; . \tag{10}$$

The associated Legendre polynomials for negative m are defined as

$$P_n^m(x) = P_n^{-M}(x) = (-1)^M \frac{(n+m)!}{(n-m)!}P_n^M(x) \; . \tag{11}$$

The coefficients a_{nm} are determined by the integration

$$a_{nm} = \int_0^{2\pi}\int_0^{\pi} r(\eta,\varphi)\sin(\eta)\bar{Y}_n^m(\eta,\varphi)d\eta d\varphi \; , \tag{12}$$

where $\bar{Y}_n^m(\eta,\varphi)$ is the complex conjugate to $Y_n^m(\eta,\varphi)$. The analytical evaluation of a_{nm} is practically not affordable (except for the case of a sphere where a_{00} is the only nonzero coefficient) and it is therefore necessary to apply a numerical integration. This requires that the values of the searched function $r(\eta,\varphi)$ are available at integration points in advance. In the presented study, the Gaussian numerical integration is employed. Theoretically, the order of the numerical integration should approach infinity. However, taking for the approximation of $r(\eta,\varphi)$ the final summation

$$r(\eta,\varphi) = \sum_{n=0}^{N}\sum_{m=-n}^{n} a_{nm}Y_n^m(\eta,\varphi) \; , \tag{13}$$

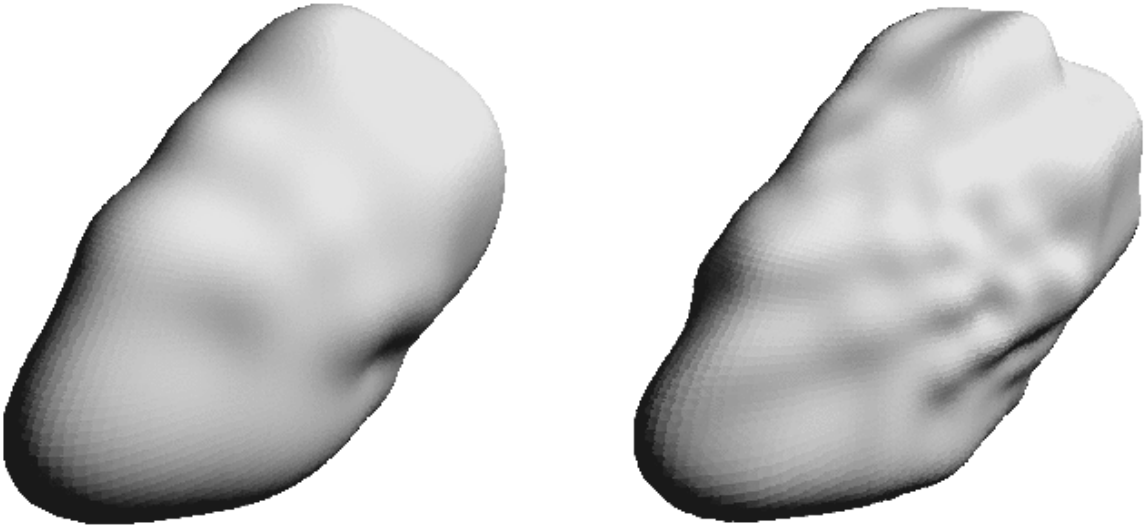

Figure 3: Representation of the aggregate particle by the spherical harmonic expansion of order 10 (left) and 20 (right).

where N is the order of the expansion, the order of the numerical integration needed for accurate evaluation of coefficients a_{nm} and consequently also the number of values $r(\eta, \varphi)$ known a priori is reduced. In the present work, the value $r(\eta, \varphi)$ at integration point is determined as the length of the segment in the direction given by η and φ connecting the center of mass with the surface of the voxel forming the aggregate boundary (see Figure 2 on the right).

The numerical experiments reveal that contributions of the expansion terms for $n > 20$ are usually negligible and that the order 128 of Gaussian numerical integration is sufficient in most cases. It is also important to realize that the growth of the expansion order may lead instead of the expected improvement of the geometrical representation to the undesirable capturing of the unrealistic digital roughness inherently comprised in the voxel based description. An example of the representation of the aggregate particle using the spherical harmonic expansion with 128-point Gaussian numerical integration (the digital representation from Figure 1 with the higher resolution was taken as the input) is shown in Figure 3 for two different values of N (10 and 20).

4. Evaluation of Geometrical Properties

After the spherical harmonic analysis is completed, the aggregate particle in a general location is represented by the origin and unit vectors corresponding to the positive x, y, and z axes of the local spherical coordinate system used for the spherical harmonic expansion, by the order of the expansion, and by the set of expansion coefficients. For the actual evaluation of geometrical properties only the last two parameters, the order of the expansion and the expansion coefficients, are relevant. The remaining parameters describe the spatial location of the aggregate particle and may be used for evaluation of some of the geometrical properties in the global Cartesian coordinate system.

The analytical expression of the volume of the aggregate particle is given by

$$V = \int_V dxdydz = \int_0^{2\pi}\int_0^{\pi}\int_0^{r(\eta,\varphi)} J(\eta,\varphi)drd\eta d\varphi = \tag{14}$$

$$= \int_0^{2\pi}\int_0^{\pi}\int_0^{r(\eta,\varphi)} r^2(\eta,\varphi)\sin(\eta,\varphi)drd\eta d\varphi = \frac{1}{3}\int_0^{2\pi}\int_0^{\pi} r^3(\eta,\varphi)\sin(\eta,\varphi)d\eta d\varphi \ ,$$

where J is the Jacobian of the transformation from the Cartesian coordinate system to the spherical coordinate system represented by Eqs. (1) – (3). The components of inertia tensor I_{ij}, where $i,j = x,y,z$, are defined as

$$I_{ij} = \int\limits_V (\delta_{ij} r^2(\eta,\varphi) - ij)dxdydz \ , \tag{15}$$

where δ_{ij} is the Kronecker delta. After inserting for x, y, and z from Eqs. (1) – (3) and performing the integration in r, the individual moments of inertia yield

$$I_{xx} = \frac{1}{5}\int_0^{2\pi}\int_0^{\pi} r^5\sin(\eta)(1-\sin^2(\eta)\cos^2(\varphi))d\eta d\varphi \ , \tag{16}$$

$$I_{yy} = \frac{1}{5}\int_0^{2\pi}\int_0^{\pi} r^5\sin(\eta)(1-\sin^2(\eta)\sin^2(\varphi))d\eta d\varphi \ , \tag{17}$$

$$I_{zz} = \frac{1}{5}\int_0^{2\pi}\int_0^{\pi} r^5\sin^3(\eta)d\eta d\varphi \ , \tag{18}$$

$$I_{xy} = I_{yx} = -\frac{1}{5}\int_0^{2\pi}\int_0^{\pi} r^5\sin^3(\eta)\sin(\varphi)\cos(\varphi)d\eta d\varphi \ , \tag{19}$$

$$I_{yz} = I_{zy} = -\frac{1}{5}\int_0^{2\pi}\int_0^{\pi} r^5\sin^2(\eta)\cos(\eta)\cos(\varphi)d\eta d\varphi \ , \tag{20}$$

$$I_{zx} = I_{xz} = -\frac{1}{5}\int_0^{2\pi}\int_0^{\pi} r^5\sin^2(\eta)\cos(\eta)\sin(\varphi)d\eta d\varphi \ . \tag{21}$$

Note that these moments are related to axes passing through the center of expansion which corresponds to the center of mass evaluated from the digital representation but which is likely to be different from the center of mass associated with the spherical harmonic expansion. Therefore, Steiner's proposition has to be applied when central moments of inertia are to be calculated.

For the evaluation of the surface area and local curvature (at a point), the first and second derivatives of $r(\eta,\varphi)$ with respect to η and φ have to be computed at first. With the help of the recursive relation [Weisstein]

$$\frac{dP_n^m(\cos(\eta))}{d\eta} = \frac{n\cos(\eta)P_n^m(\cos(\eta)) - (n+m)P_{n-1}^m(\cos(\eta))}{\sqrt{1-\cos^2(\eta)}} \tag{22}$$

they can be expressed in the form

$$r_\eta = \sum_{n=0}^{N}\sum_{m=-n}^{n} \frac{-a_{nm}f_{nm}}{\sin(\eta)} A_{nm}(\eta)(\cos(m\varphi) + i\sin(m\varphi)) \ , \tag{23}$$

$$r_\varphi = \sum_{n=0}^{N}\sum_{m=-n}^{n} ima_{nm}Y_n^m(\eta,\varphi) \ , \tag{24}$$

$$r_{\eta\eta} = \sum_{n=0}^{N}\sum_{m=-n}^{n} \frac{a_{nm}f_{nm}}{\sin^2(\eta)} B_{nm}(\eta)(\cos(m\varphi) + i\sin(m\varphi)) \ , \tag{25}$$

$$r_{\varphi\varphi} = \sum_{n=0}^{N}\sum_{m=-n}^{n} -m^2a_{nm}Y_n^m(\eta,\varphi) \ , \tag{26}$$

$$r_{\eta\varphi} = r_{\varphi\eta} = \sum_{n=0}^{N} \sum_{m=-n}^{n} \frac{-ima_{nm}f_{nm}}{\sin(\eta)} C_{nm}(\eta)(\cos(m\varphi) + i\sin(m\varphi)) \,, \tag{27}$$

where the auxiliary quantities $A_{nm}(\eta)$, $B_{nm}(\eta)$, and $C_{nm}(\eta)$ read

$$A_{nm}(\eta) = [(n+1)\cos(\eta)P_n^m(\cos(\eta)) - (n-m+1)P_{n+1}^m(\cos(\eta))] \,, \tag{28}$$

$$\begin{aligned} B_{nm}(\eta) \;=\; & [(n+1+(n+1)^2\cos^2(\eta))P_n^m(\cos(\eta)) - \\ & - 2(n+2)(n-m+1)\cos(\eta)P_{n+1}^m(\cos(\eta)) + \\ & + (n-m+1)(n-m+2)P_{n+2}^m(\cos(\eta))] \,, \end{aligned} \tag{29}$$

$$C_{nm}(\eta) = [(n+1)\cos(\eta)P_n^m(\cos(\eta)) - (n-m+1)P_{n+1}^m(\cos(\eta))] \,. \tag{30}$$

The above derivatives are used for the evaluation of the first and second gradients of $\boldsymbol{r}$ with respect to η and φ according to

$$\begin{aligned} \boldsymbol{r}_\eta \;=\; & \{(r_\eta\sin(\eta) + r\cos(\eta))\cos(\varphi) \;, \\ & (r_\eta\sin(\eta) + r\cos(\eta))\sin(\varphi) \,, \\ & r_\eta\cos(\eta) - r\sin(\eta)\}^T \;, \end{aligned} \tag{31}$$

$$\begin{aligned} \boldsymbol{r}_\varphi \;=\; & \{(r_\varphi\cos(\varphi) - r\sin(\varphi))\sin(\eta) \;, \\ & (r_\varphi\sin(\varphi) + r\cos(\varphi))\sin(\eta) \,, \\ & r_\varphi\cos(\eta)\}^T \;, \end{aligned} \tag{32}$$

$$\begin{aligned} \boldsymbol{r}_{\eta\eta} \;=\; & \{(r_{\eta\eta}\sin(\eta) + 2r_\eta\cos(\eta) - r\sin(\eta))\cos(\varphi) \;, \\ & (r_{\eta\eta}\sin(\eta) + 2r_\eta\cos(\eta) - r\sin(\eta))\sin(\varphi) \,, \\ & r_{\eta\eta}\cos(\eta) - 2r_\eta\sin(\eta) - r\cos(\eta)\}^T \;, \end{aligned} \tag{33}$$

$$\begin{aligned} \boldsymbol{r}_{\varphi\varphi} \;=\; & \{(r_{\varphi\varphi}\cos(\varphi) - 2r_\varphi\sin(\varphi) - r\cos(\varphi))\sin(\eta) \;, \\ & (r_{\varphi\varphi}\sin(\varphi) + 2r_\varphi\cos(\varphi) - r\sin(\varphi))\sin(\eta) \,, \\ & r_{\varphi\varphi}\cos(\eta)\}^T \;, \end{aligned} \tag{34}$$

$$\begin{aligned} \boldsymbol{r}_{\varphi\eta} \;=\; & \{(r_{\eta\varphi}\cos(\varphi) - r_\eta\sin(\varphi))\sin(\eta) + (r_\varphi\cos(\varphi) - r\sin(\varphi))\cos(\eta) \;, \\ & (r_{\eta\varphi}\sin(\varphi) + r_\eta\cos(\varphi))\sin(\eta) + (r_\varphi\sin(\varphi) + r\cos(\varphi))\cos(\eta) \,, \\ & r_{\eta\varphi}\cos(\eta) - r_\varphi\sin(\eta)\}^T \;, \end{aligned} \tag{35}$$

from which the coefficients of the first (E, F, G) and second (L, M, N) fundamental forms of the surface are calculated as

$$E = \boldsymbol{r}_\eta \cdot \boldsymbol{r}_\eta \,, \quad F = \boldsymbol{r}_\eta \cdot \boldsymbol{r}_\varphi \,, \quad G = \boldsymbol{r}_\varphi \cdot \boldsymbol{r}_\varphi \,, \tag{36}$$

$$L = \boldsymbol{r}_{\eta\eta} \cdot \boldsymbol{n} \,, \quad M = \boldsymbol{r}_{\eta\varphi} \cdot \boldsymbol{n} = \boldsymbol{r}_{\varphi\eta} \cdot \boldsymbol{n} \,, \quad N = \boldsymbol{r}_{\varphi\varphi} \cdot \boldsymbol{n} \,, \tag{37}$$

where the unit surface outer normal vector $\boldsymbol{n}$ is given by

$$\boldsymbol{n} = \frac{\boldsymbol{r}_\eta \times \boldsymbol{r}_\varphi}{\sqrt{EG - F^2}} \,. \tag{38}$$

The total surface area S is defined as

$$S = \int_0^{2\pi}\int_0^{\pi} dS \,, \tag{39}$$

where the differential surface area dS reads

$$dS = r\sqrt{r_\varphi^2 + (r_\eta^2 + r^2)\sin^2(\eta)}\, d\eta d\varphi = \sqrt{EG - F^2}\, d\eta d\varphi \,. \tag{40}$$

The principal curvatures κ_1 and κ_2 at the surface point are given by the solution of the quadratic equation

$$(EG - F^2)\kappa_{12}^2 + (EN - 2FM + GL)\kappa_{12} + (LN - M^2) = 0 \,. \tag{41}$$

Two local measures of the surface curvature are derived from the principal curvatures. While the local mean curvature H is defined as the arithmetical mean of the two principal curvatures

$$H = \frac{\kappa_1 + \kappa_2}{2} = \frac{EN - 2FM + GL}{2(EG - F^2)} \,, \tag{42}$$

the local Gaussian curvature K is given by the square of their geometric mean

$$K = \kappa_1\kappa_2 = \frac{LN - M^2}{EG - F^2} \,. \tag{43}$$

The corresponding global measures, the average mean curvature h and the average Gaussian curvature k, are then defined as

$$h = \frac{1}{S}\int_0^{2\pi}\int_0^{\pi} H dS \,, \tag{44}$$

$$k = \frac{1}{4\pi}\int_0^{2\pi}\int_0^{\pi} K dS \,. \tag{45}$$

Note that all the above integral values have to be evaluated numerically (again with the exception of a sphere, in which case the analytical evaluation is affordable). In the presented work, the Gaussian quadrature is adopted. Since the average Gaussian curvature is equal to one for all objects topologically equivalent to a sphere, which is the case of aggregate particles and their spherical harmonic representations considered in this work, it can be effectively used as a control tool for setting up the order of the numerical integration scheme used for the evaluation of the geometrical properties. The numerical experiments again reveal that the integration order 128 is accurate enough in most cases.

5. Performance and examples

The above approach for the evaluation of geometrical properties is firstly verified on shapes with known analytical results for their properties. The first candidate, a sphere, is however too trivial to be used for that purpose. The other choice is the ellipsoid of revolution whose properties can be also derived in the analytical form using elementary functions. Initially, two ellipsoids centered at the origin and aligned with the coordinate axes with z axis being the axis of revolution were investigated. Similarly as in [Garboczi 2002], prolate and oblate ellipsoids with the axes in the ratio 1:1:5 and 5:5:1 were considered at first. The spherical harmonic expansion coefficients, however, were obtained from the exact formulas without realizing a particular

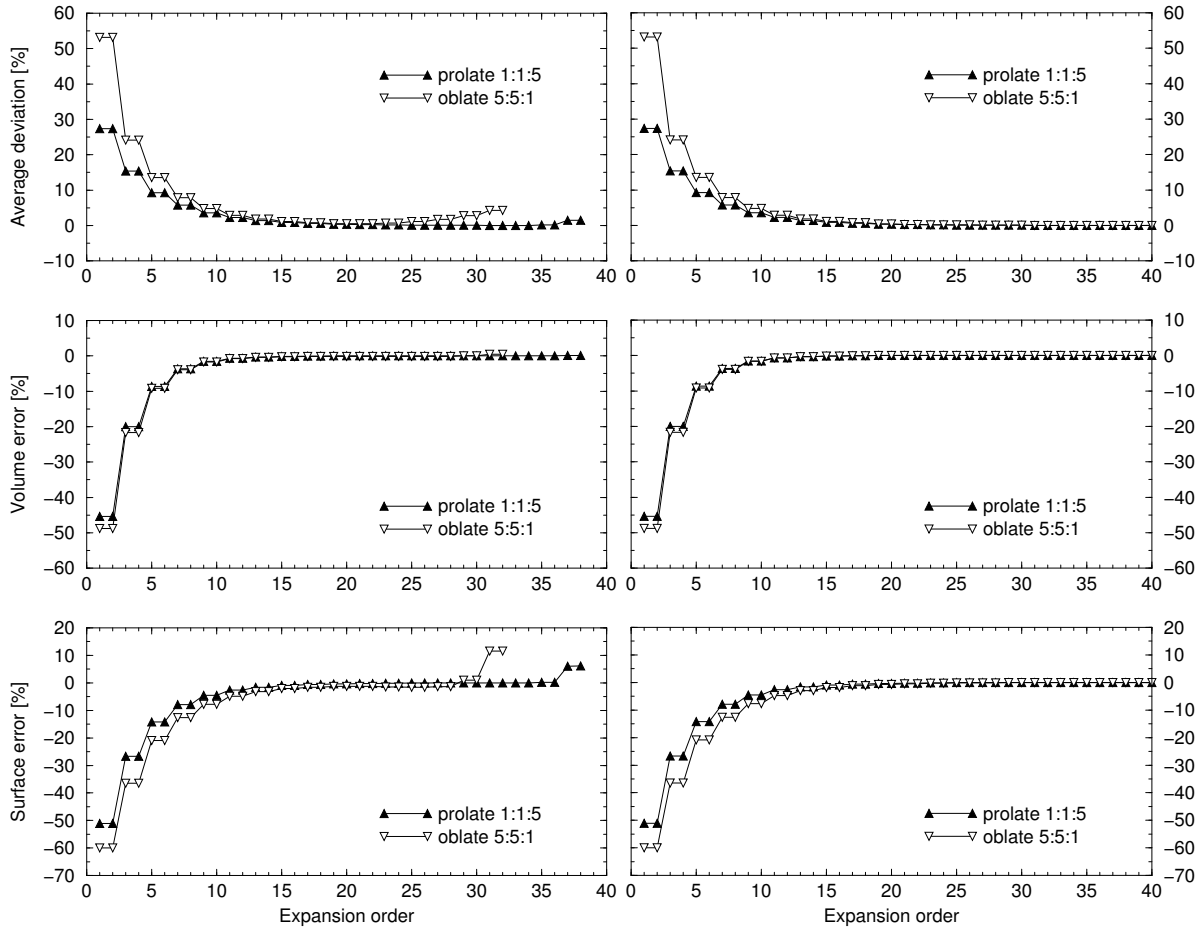

Figure 4: Dependence of the average deviation (top row), volume error (middle row), and surface area error (bottom row) on the expansion order for integration order 64 (left column) and 128 (right column). The represented object is a prolate (1:1:5) and an oblate (5:5:1) ellipsoid of revolution.

digital representation. Except the volume and surface area, the quality of the expansion is assessed using additional quantity, the average deviation from the exact shape, defined as

$$\delta = \frac{1}{S}\int_0^{2\pi}\int_0^{\pi}\frac{|r - r_{ex}|}{r_{ex}}dS\ , \tag{46}$$

where r_{ex} is the exact value corresponding to $r(\eta, \varphi)$. The dependence of the average percentage deviation of the spherical harmonic expansion from the exact shape as well as the percentage error of the volume and surface area evaluated from the spherical harmonic expansion on the number of expansion terms is depicted in Figure 4 for two different integration orders (64 and 128) used for the spherical harmonic analysis. For the evaluation of the geometrical properties, integration scheme of order 256 was always applied. Note that since the range spanned by η is of half size compared to the size of range spanned by φ, the integration order in η direction is always reduced to the half. The profiles in Figure 4 show, that the evaluated geometrical quantities are rapidly converging to exact values with expansion order increasing up to the value about 20. When the expansion order is further increased, the behaviour depends on the integration order used for the spherical harmonic analysis. If the adopted integration scheme

Figure 5: Oscillations on the oblate ellipsoid for the expansion order 32 and the integration order 64.

Figure 6: Artificial object with 5 waves passing around the object body from top to bottom.

is of sufficiently high order, the quantities remain to converge. For a low order integration scheme, however, the approximation property of the spherical harmonic analysis vanishes and the analysis starts to behave as an interpolating scheme resulting in oscillations around the exact shape (see Figure 5). This is evident from the growth of the surface area error and from the increasing average deviation which are the direct consequence of these oscillations. On the other hand, the evaluation of the volume seems to be not affected by this effect (at least immediately), which can be explained by approximately the same increment and decrement of the volume due to the oscillation. The step-wise character of the profiles in Figure 4 is the consequence of the fact, that $r(\eta, \varphi)$ (for both considered ellipsoids) is independent of φ and is even in η. This implies that the only nonzero spherical harmonic coefficients a_{nm} are those with n even and $m = 0$. Incrementing the odd expansion order by one does not therefore introduce any new nonzero expansion coefficient while keeping the existing coefficients at the same value. All geometrical quantities thus remain unchanged. Similar profiles are observed also for ellipsoids with the axis of revolution aligned with x or y axes. This suggests that the integration order should be at least twice as large as the required expansion order.

The next considered object is rather of artificial shape (see Figure 6) given by Eqs. (1) – (3) with $r(\eta, \varphi)$ defined as

$$r(\eta, \varphi) = 5(1 + 2\sin^2(\eta))(1 + 0.1\sin(\eta)\cos(w(\varphi + 2\eta))) \tag{47}$$

where w is the number of waves passing around the object body from top to bottom. Two particular examples with 5 and 10 waves were investigated. The dependence of the average percentage deviation of the spherical harmonic expansion from the exact shape and of the percentage error of the volume and surface area evaluated from the spherical harmonic expansion on the number of expansion terms is displayed in Figure 7 again for two different integration orders (64 and 128) used for the spherical harmonic analysis. This time, however, the exact volume and surface area are not known and therefore they are approximated by numerical values obtained from a fine tessellation (1000 in η x 2000 in φ) of the exact shape. Qualitatively, the obtained results reveal similar behaviour to that observed for ellipsoids. From the quantitative point of view, there are some differences. First of all, when treating the object with 10 waves, 64-point integration is not enough to assess the surface area. When 128-point integration

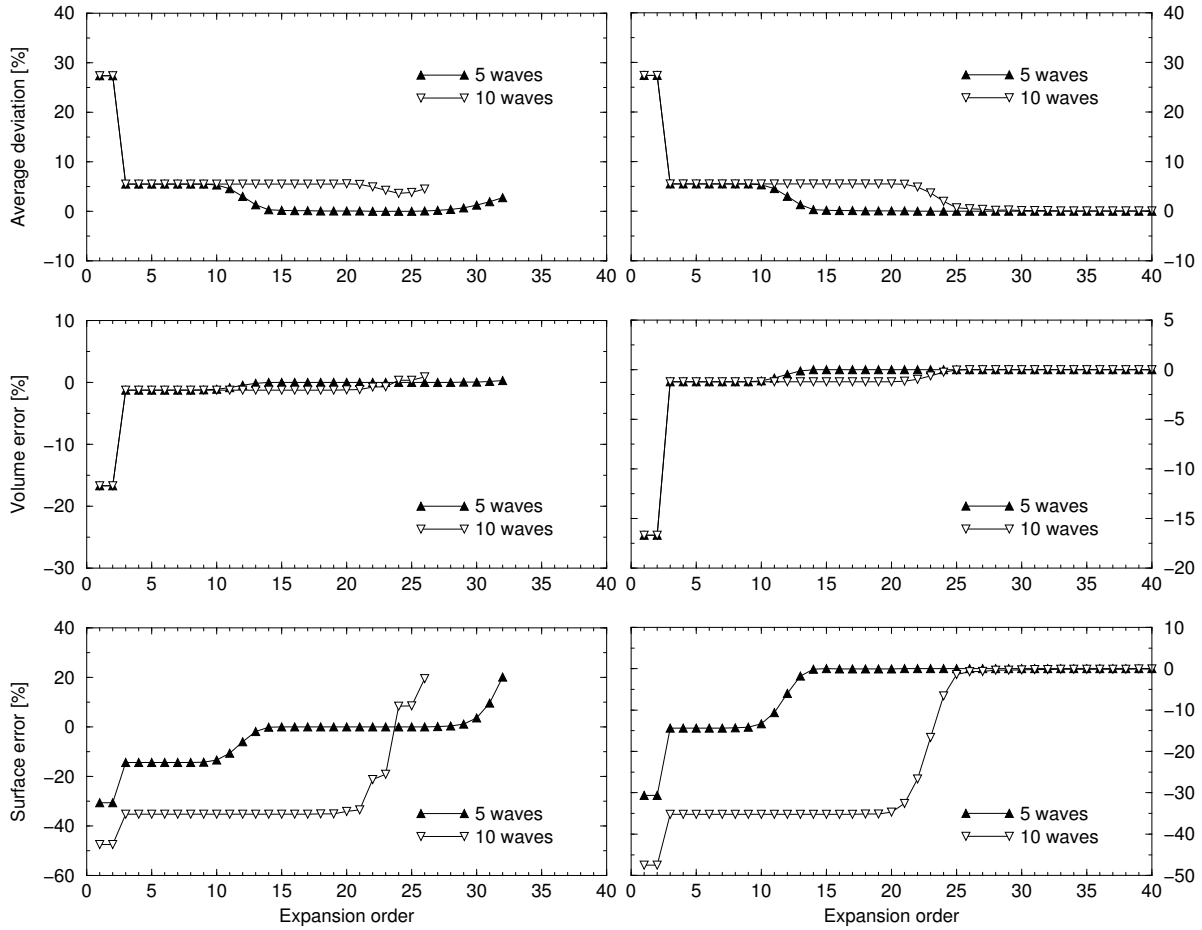

Figure 7: Dependence of the average deviation (top row), volume error (middle row), and surface area error (bottom row) on the expansion order for integration order 64 (left column) and 128 (right column). The represented object is the artificial shape with 5 and 10 waves.

scheme is applied, the expansion order of at least 25 should be used to achieve reasonable accuracy. The step-wise profiles experienced for ellipsoids are replaces by a plateau-like profiles, where the length of the plateau is related to the number of waves that have to be captured by the spherical harmonic functions.

Finally, the geometrical properties were evaluated for the aggregate particle presented in Sections 2 and 3. The digital representation shown in Figure 1 on the right was considered. Since the exact shape of the aggregate particle is unknown, only the evolution of the volume and surface area in dependence on the expansion order is shown. In Figure 8, these profiles are presented for four different integration orders (32, 64, 128, and 256). While the volume converges to a constant value (corresponding to the volume calculated from the voxel based representation), the surface area is monotonically increasing on the whole range of adopted expansion orders. This can be explained by the fact that the spherical harmonic expansion tends with the growing expansion order to capture better and better the unrealistic voxel based geometry, which increases the surface area toward (or even beyond) the bad value corresponding to the digital surface area. It is therefore quite difficult to determine how many expansion terms should be used to get the most realistic results. Unfortunately, the most reliable prompt, so far, seems to be the visual inspection of the geometrical shape represented by the spherical

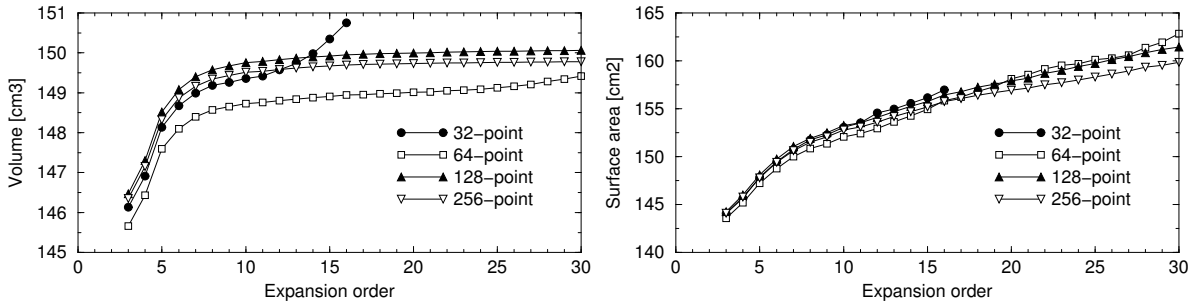

Figure 8: Dependence of the aggregate particle volume (left) and surface area (right) on the expansion order for 32-, 64-, 128-, and 256-point integration scheme.

harmonic expansion of a particular order (see Figure 3). The Figure 8 also reveals, that there is a relatively significant error in the evaluated volume for 64-point integration scheme. It is, however, not clear what is causing this aspect.

6. Conclusions

The description of geometrical shapes using the spherical harmonic expansion offers a flexible and powerful tool for the representation of aggregate particles. Contrary to the digital voxel based representation, it is much less memory demanding and enables a simple and reliable evaluation of geometrical properties such as volume, moments of inertia, surface area, and curvature. These properties can be used for the classification of aggregate particles according to their morphological aspects and eventually for building an aggregate database. The smooth representation based on the spherical harmonic analysis also allows incorporation of aggregate particles into various computational models, because aggregate particles can be subjected to spatial discretization of appropriate resolution [Rypl 2006].

7. Acknowledgments

This work was supported by the Grant Agency of Czech Republic project No. 103/05/2315. Its financial assistance is gratefully acknowledged.

8. References

[Garboczi 2002] Garboczi, E.J. 2002: Three-dimensional mathematical analysis of particle shape using X-ray tomography and spherical harmonics: Application to aggregate used in concrete. *Cement and Concrete Research*, vol. 32, 1621–1638.

[Rypl 2006] Rypl, D. 2006: Discretization of three-dimensional aggregate particles. To be presented at the Third European Conference on Computational Mechanics Solids, Structures and Coupled Problems in Engineering held in Lisabon in June 2006.

[Weisstein] Weisstein, E.W.: Legendre polynomial. MathWorld Web Resource. http://mathworld.wolfram.com/LegendrePolynomial.html